Producing and Characterization of Free-Standing SnO$_2$/Graphene Composite Anodes for Li-Ion Batteries

*[1]Hilal Köse, [1]Şeyma Dombaycıoğlu, [2]Hatem Akbulut and [1]Ali Osman Aydın
*[1]Department of Chemistry, Faculty of Arts&Sciences, Sakarya University, Turkey
*[2]Department of Metallurgy and Material Engineering, Faculty of Engineering, Sakarya University, Turkey

Abstract

Free-standing SnO$_2$ / Graphene (G) nanocomposite anode materials are new high capacity anode materials for lithium ion batteries. This structure was fabricated by using SnO$_2$ nanopowders synthesized via microwave-assisted hydrothermal technique and graphene oxide synthesized via Hummers' method. The weight ratio effect of SnO$_2$ nanopowders / GO on the anode structure and electrochemical behavior was investigated. Produced SnO$_2$ / Reduced Graphene Oxide (rGO) nanocomposites were characterized by scanning electron microscopy (SEM), energy dispersive X-ray spectrometer (EDS), and X-ray diffraction (XRD) analyses. After 50 cycles of electrochemical test, the cell assembled with 1:1 and 2:1 (w/w) SnO$_2$/rGO free-standing anodes showed 578 and 530 mAh g^{-1} discharge capacities, respectively. The results indicated that the SnO$_2$/rGO composite produced by vacuum filtration is suitable for applying as an anode electrode for Li-ion batteries to increase electrochemical energy storage performance.

Key words: Li-ion battery anodes, SnO$_2$/G nanocomposites, microwave-assisted hydrothermal synthesis, vacuum filtration, electrochemical characterization.

1. Introduction

Lithium-ion batteries have attracted considerable attention in science and industry fields with high reversible capacity, long cycle life, and low cost. Graphite is the most popular anode material in commercial LIBs anodes and shows superb cyclability, but low capacity (372 mAh g^{-1}) negatively affects its industrial applications [1].

Metal oxides have attracted much attention due to their higher theoretical capacities and higher energy densities than those of conventional graphite anodes. Among them, tin dioxide (SnO$_2$) has a high specific capacity (1491 mAh g^{-1}) and is considered as one of the most suitable materials to replace the carbon anode in the lithium-ion battery. However, large volume expansion and agglomeration occur in the structure of SnO$_2$ during the Li-ion insertion and extraction process, which leads to failure and loss of electrical contact of the anode [2].

To prevent these reasons of capacity failure, graphene is used to provide buffering effect against the volume changes during the delithiation/lithiation by forming nanocomposite structure with SnO$_2$ [3]. Graphene is one of the thinnest materials in universe with a two-dimensional carbon sheet with one atom thickness. Graphene has unique electronic, mechanical, optical, thermal, and chemical properties which are inherited from the two-dimensional atomic structures. Therefore, graphene nanocomposites or hybrids are attracting increasing efforts for real applications in energy aspects by introducing controlled functional building blocks to graphene [4]. Also, free-

*Corresponding author: Address: Department of Chemistry, Faculty of Arts&Sciences, Sakarya University, 54187, Sakarya TURKEY. E-mail address: hkose@sakarya.edu.tr, Phone: +902642955938

standing buckypaper consisted of rGO are thought to prevent the pulverization of the anode structure and capacity fading due to its outstanding properties.

In this work, the synthesis and characterization of SnO_2/G nanocomposites were studied to obtain high capacity anode materials. Firstly, SnO_2 powders were synthesized by microwave-assisted hydrothermal method using glycerin additive to form a mesoporous structure. Then, free-standing anodes were produced by ultrasonication of the 1:1 and 2:1 (w/w) mixture of GO (Hummers' method) and SnO_2, respectively. After vacuum filtration, the SnO_2/GO papers were peeled off from the PVDF membrane, reduced in hydrazine hydrate solution and obtained SnO_2/rGO structures as anode in CR2016 Li-ion cell. The weight ratio effect of SnO_2 nanopowders and GO on the anode structure and electrochemical behavior was also investigated.

Produced SnO_2/rGO nanocomposites were characterized by SEM, EDS and XRD analyses. CR2016 cells were charged and discharged at 25 °C between fixed voltage limits (2.5 V to 0.01 V) at a constant current density on a BST8-MA MTI model battery tester. Cyclic voltammetry (CV) was carried out for the anode over the potential range of 2.5–0.01 V vs. Li/Li$^+$ at a scanning rate of 0.1 mV s^{-1}

2. Materials and Method

2.1. Preparation of SnO₂/rGO buckypaper nanocomposites

To produce SnO_2/rGO buckypaper nanocomposites, firstly graphene oxide was synthesized from pre-treated graphite powders via modified Hummers' method. For the pretreatment process, 1.0 g of pristine graphite powder was exposed to 50 mL of HNO_3/H_2SO_4 (nitric acid 65%, and sulfuric acid 95–97%) (volume ratio of 1:3) solution under vigorous stirring for 2 h and then washed with distilled water until pH becomes neutral and dried in air at 70 °C for 24 h. After drying the product, it was subsequently heat treated in air atmosphere at 850 °C for 120 s. For the graphite oxide production, 1.0 g of pre-treated graphite powder and 0.5 g $NaNO_3$ (Sigma–Aldrich, ≥ 99.0%) were added into 23 mL of H_2SO_4 acid and stirred for 2 h by magnetic stirrer until a homogenous mixture was obtained. The mixture was then cooled down to 0 °C by using an ice bath and 3.0 g $KMnO_4$ was added slowly into the mixture while keeping the reaction temperature below 20 °C. After addition of $KMnO_4$, the ice bath was removed and the mixture was heated up to 35 °C for 30 min. 46 mL deionized H_2O was slowly added into the mixture and the temperature was increased to 98 °C due to exothermic reaction and it was kept at 98 °C for 15 min to maintain the reaction temperature. Next, 140 mL of hot water and then 10 mL H_2O_2 aqueous solution were added into the mixture and a homogeneous suspension was obtained with dark yellow color after stirring the mixture for 2 h. Further, the product washed with distilled water and centrifuged until pH become neutral. The product was dried at 60 °C in vacuum oven and graphite oxide was obtained as literature [5].

To produce graphene oxide and its nanocomposite with SnO_2, graphite oxide was exfoliated by ultrasonication together SnO_2 nanopowders. To produce 1:1 and 1:2 ratio of SnO_2/GO, 45 mg and 22.5 mg microwave-assisted hydrothermal synthesized SnO_2 was dispersed with 45 mg of as-synthesized graphite oxide in 50 mL of distilled water and sonicated for 2 h to increase the

interlayer distances between graphite oxide layers to obtain graphene oxide. Then, the solution was filtered on PVDF membrane (Millipore, Durapore Membrane) by vacuum filtration technique. Then, after vacuum filtration, the SnO_2/GO paper was peeled off from the PVDF membrane, reduced in distilled hydrazine solution. SnO_2/rGO free-standing paper was obtained and used as anode in CR2016 Li-ion cell.

For the production of microwave-assisted SnO_2 nanopowders by hydrothermal method, 0.003 mole $SnCl_2.2H_2O$ (tin (II) chloridedihydrate) and 0.03 mole glycerin were dissolved in water and then NH_3 (25%) solution was added in suspension which is in a Teflon vessel. Milestone microwave furnace was used for the synthesis of powders at the experimental conditions of 160 °C and 500 W. After 2 hours the products were washed via centrifugation (8000 rpm) with water for several times. Obtained precipitations firstly dried at 100 °C and then calcined at 700 °C for 2 hours in an ash oven at air atmosphere.

2.2. Physical characterization of materials

The structure of the free-standing nanocomposite was analyzed by scanning electron microscopy SEM (SEM-JEOL-JSM 6060LV). The chemical composition of the composite was determined by energy dispersive X-ray spectrometer (EDS) attached to the SEM. The working conditions for EDS analysis include an accelerating voltage of 15 kV, a beam current of 5 nA, a working distance of 15 mm, and a live time of 60 s for each run. XRD analysis was performed with X-ray diffractometer (Rigaku D/MAX/2200/PC model device) using CuKα radiation (λ= 1.54050 Å) with 1°/ min scanning speed using a grazing angle of 5°.

2.3. Electrochemical cell preparation and measurements

The SnO_2/rGO buckypaper nanocomposite anodes were used as working electrode. Metallic lithium and polypropylene (PP) were used as cathode and separator, respectively. The commercial electrolyte consisting of a 1.0 M solution of $LiPF_6$ dissolved in a 50:50 mixture by volume of ethylene carbonate (EC) and dimethyl carbonate (DMC) was used. CR2016 cells were assembled in a glove box (MBraun-Labstar). The cells were charged and discharged at 25 °C between fixed voltage limits (2.5 V to 0.01 V) at a constant current density on a BST8-MA MTI model battery tester. The charge discharge rate was chosen as 0.2C for discharge capacity measurements. Cyclic voltammetry (CV) was performed at the scan rate of 0.1 mVs^{-1}.

3. Results and Discussion

3.1. Structural characterization

SEM microstructures of the produced GO and rGO buckypaper surface are given in Figure 1(a) and (b). SEM back-scattered micrographs of these buckypaper structures with cross-section are clearly indicated graphene oxide and reduced graphene oxide sheets at high magnification in Figure 1(c) and (d), respectively. The cross-sectional SEM images of the papers show that the GO and rGO sheets have a suitable porosity for Li$^+$ diffusion improving the efficiency of the alloying-dealloying of Li-Sn. Additionally, the structures seem to exhibit a mesoporous nature

with a homogeneous distribution of sheets, which is targeted to obtain for anode in Li batteries to accommodate stresses arisen from the volume change during charging and discharging [6]. The papers peeled off from the polyvinylidene fluoride membrane indicate a flexible, free-standing structure.
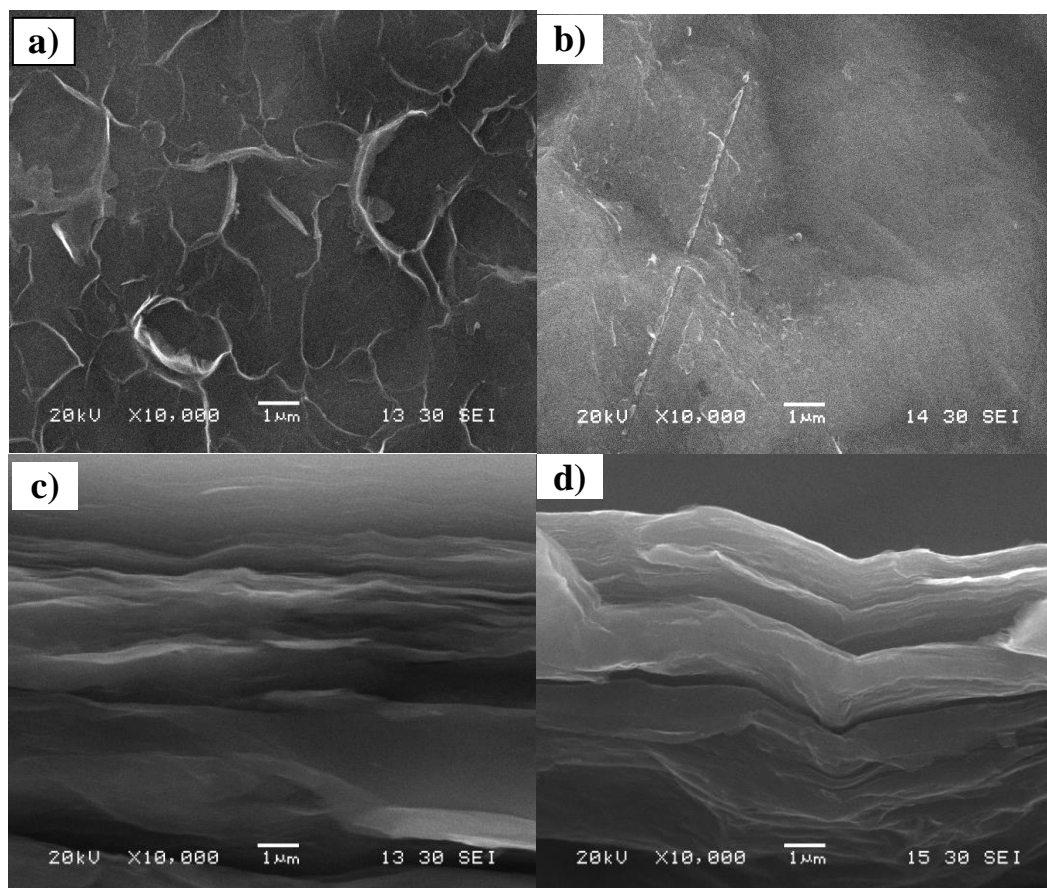

Figure 1. SEM image of a) GO, b) rGO paper surface and cross- sectional c) GO, d) rGO.

Figure 2(a) and 2(b) show the SEM surface images of 1:1 and 1:2 SnO_2/rGO nanocomposites, respectively. When we compare the structures, the surface of 1:1 SnO_2/rGO composite seems wavier than 1:2 composite. It may be due to using more SnO_2 powders for 1:1 composite. The images show that there is no SnO_2 agglomeration on the surfaces. Also, SnO_2 nanoparticles can be seen under the graphene layers. As a result, a desired cracks-free structure was obtained to prevent mechanical disintegration of the anode with a homogeneous distribution of SnO_2 nanoparticles.
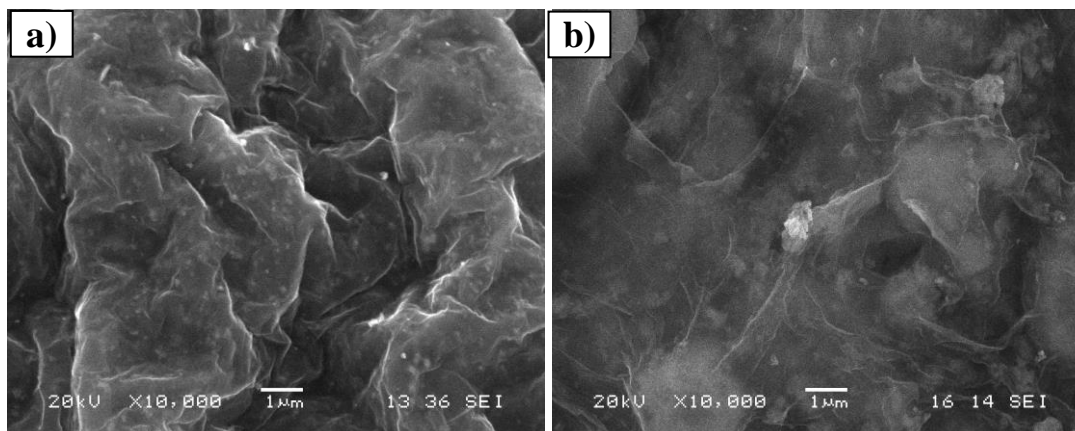
Figure 2. SEM image of the surface of a) 1:1 SnO_2/rGO and b) 1:2 SnO_2/rGO composites.

Figure 3 shows EDS elemental mappings with a typical SEM image besides the corresponding C, Sn and O maps for the SnO_2/rGO composites. They reveal the SnO_2 particle nucleation and growth on the graphene sheets. As can be seen from the figures, C, Sn and O elements show very homogeneous distribution, indicating that Sn possesses a good penetration into the sheets.
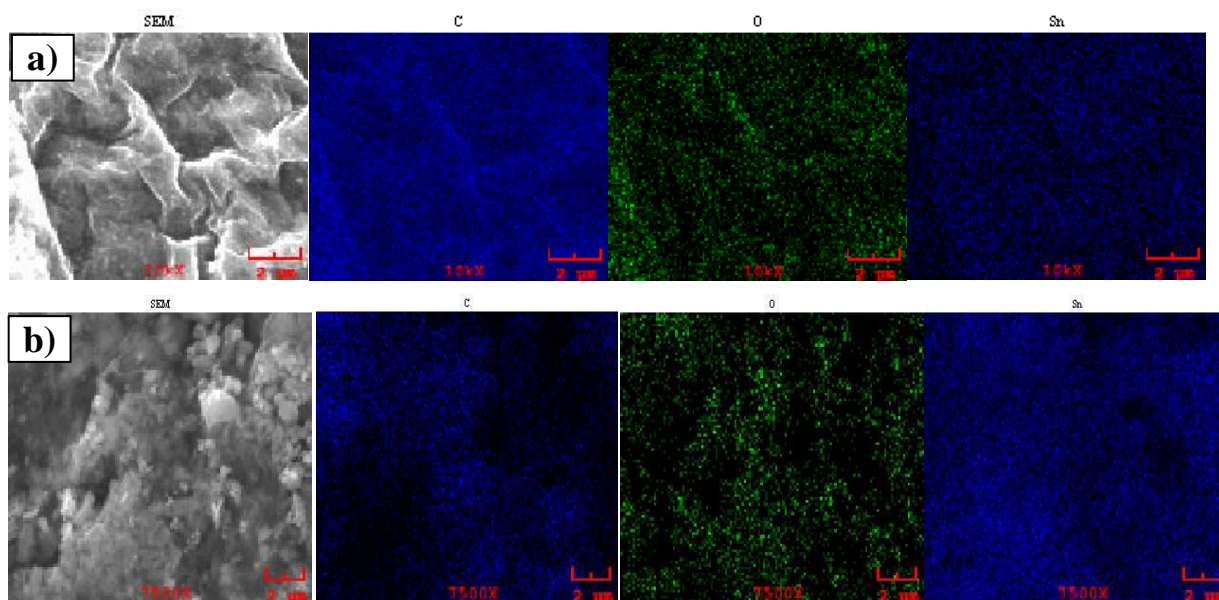

Figure 3. Elemental mapping of a) 1:1 SnO_2/rGO, b) 1:2 SnO_2/rGO buckypaper nanocomposite through the SEM images and C, Sn, O elemental maps.

XRD analysis was performed to investigate the crystal structures of SnO_2/rGO buckypaper nanocomposites. Diffraction peaks of graphene oxide, graphene, SnO_2 nanopowders and SnO_2/rGO nanocomposite samples are given in Figure 4. Figure 4(a) indicates graphene oxide peak at about 11°. Normally, graphite diffraction peak is about 26°, but after oxidation, the peak shifts to 11°. It can be seen from Figure 4(b), graphene peak is at about 2θ=26° with (002) plane of carbon (JCPDS, 00-026-1080). Usually no peaks associated with graphene are detected,

although some report a peak about 26° corresponding to graphite as a result of improper preparation of graphene nanosheets. So, the main peaks of graphene oxide and graphene are almost compatible with the literature [5,7]. Pristine SnO_2 diffraction peaks (JCPDS, 00-041-1445) are given in Figure 4(c) and (110), (101), (200), (211) planes are observed. For the SnO_2/rGO nanocomposites, all of the diffraction peaks without carbon planes are about the planes of cassiterite type of SnO_2 crystal structure in Figure 4(d) and 4(e). For these composites, (002) graphene and (001) SnO_2 plane diffraction peaks are about $2\theta=26^o$ and they partially overlap.
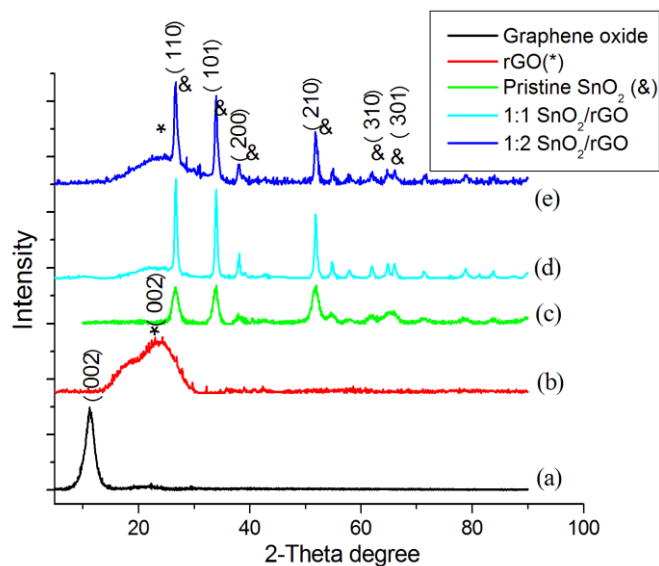

Figure 4. XRD analysis of a) GO, b) G c) pristine SnO_2 nanopowders and d) SnO_2/rGO nanocomposite buckypaper.

Debye-Scherrer formula **(Eq. 1)** is used to determine the crystal size of the SnO_2 powders used for the composite productions by using XRD data.

$$D = \frac{K \times \lambda}{\beta \times \cos\theta}$$

(Eq. 1)

In this formula, K is the shape factor (0.9), D is the mean grain size of crystalline structure, λ is the X-ray wavelength, β is the full width at half maximum (FWHM) or integral breadth of XRD peak, and θ is the Bragg angle. The crystal size of SnO_2 powders synthesized via microwave-assisted hydrothermal method was calculated according to the Scherrer formula and found as 20 nm.

3.2. Electrochemical characterization

Cyclic voltammetry (CV) measurements were performed to investigate the electrochemical properties of the SnO_2/rGO nanocomposite electrodes during the charge–discharge process. Figure 5(a) represents CVs of SnO_2/rGO nanocomposite anode of 1:1 composite. The alloying and de-alloying (intercalation) processes of lithium with SnO_2 and graphene were carried out over the potential range of 2.5–0.01 V vs. Li/Li$^+$ at a scanning rate of 0.1 mV s^{-1}.

The electrochemical reaction mechanism for the SnO_2/Li cell is described as follows [8]:

$$SnO_2 + 4Li^+ + 4e^- \longrightarrow Sn + 2Li_2O \tag{1}$$
$$Sn + xLi^+ + xe^- \rightleftarrows Li_xSn \ (0 \leq x \leq 4.4) \tag{2}$$
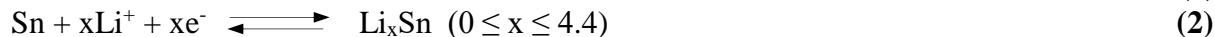
The CV curves were recorded for the SnO_2/rGO anode sample for 5 cycles. During the first discharge, an irreversible first reaction **(1)** is observed. The Li-inserted SnO_2 forms amorphous Li_2O and metallic Sn with a reduction peak (>1V) [9]. Electrochemically inactive Li_2O phase formed during the first insertion reduces the capacity of anode. The sharp and broad negative-going peak at about 0.75 V can only be observed during the first cathodic sweep, which derives from decomposition of the electrolyte and the formation of an SEI film on the anode surface [10]. The reversible reaction **(2)** of the metallic Sn with lithium subsequently leads to the formation of Li-Sn alloys with the composition of $Li_{4.4}Sn$ [11] and appears as the reduction peak below 0.5 V. The oxidation peaks at about 0.5 V can be assigned to the dealloying of Li_xSn [12]. In addition, a broad oxidation peak is found at 1.23 V, which may relate to the decomposition of Li_2O [8]. Observed reduction peak at 0.02 V and oxidation peak at 0.2 V in CVs can be attributed to lithium-ions intercalating into and extraction from the graphene layers.
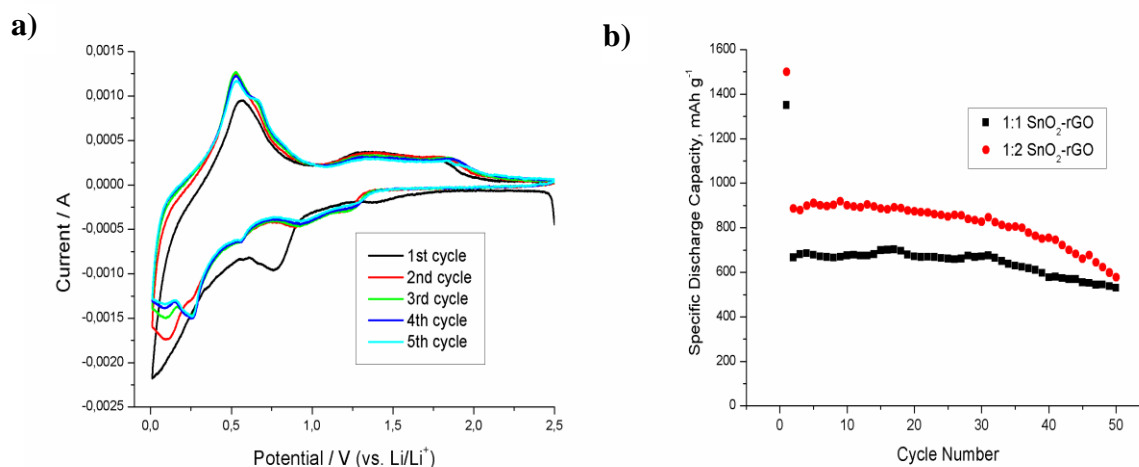

Figure 5. (a) Cyclic voltammogram curves of SnO_2/rGO anode between potential range of 2.5–0.01 V for five cycles, the scan rate is 0.1 mV s^{-1}, (b) electrochemical discharge capacity of the anodes for 50 cycles.

The comparison of discharge capacities of the SnO_2/rGO anodes is given in Table 1 and Fig 5(b). As can be seen from Table 1 and the figure, first electrochemical discharge capacities of the 1:1 and 1:2 SnO_2/rGO composite anodes are 1350 and 1500 mAh g^{-1}, respectively. For the final cycle, high discharge capacities were obtained from 1:1 and 1:2 SnO_2/rGO composite anodes as 530 and 578 mAh g^{-1}, respectively. 1:2 SnO_2/rGO composite anode indicates higher discharge capacity than 1:1 SnO_2/rGO anode for the first and final cycle. Even though 1:2 composite anode has higher capacity after 50 cycles, final capacity values are very close to each other and 1:1 composite anode has lower capacity fading than 1:2 anode, which may be due to higher quantity of SnO_2 active material.

Table 1. The comparison of discharge capacities of free-standing SnO_2/rGO buckypaper composite anodes.

Sample Name	1st Cycle (mAhg^{-1})	2nd Cycle (mAhg^{-1})	50th Cycle (mAhg^{-1})
1:1 SnO_2/rGO	1350	666	530
1:2 SnO_2/rGO	1500	886	578

As a result, free-standing 1:2 SnO_2-rGO composite anode indicated better results after 50 cycles. According to structural analysis, higher weight of SnO_2 may cause degeneration of the structure, as can be seen from Figure 2(a) SEM image of 1:1 SnO_2-rGO composite, so lower electrochemical discharge capacity is obtained. However, we can say that lower active material may affect the cycle life of the anode according to the result of the capacity fading of 1:2 SnO_2-rGO composite. Therefore, the next aim of the study will continue the charge-discharge cycle numbers of the anodes and improving of the weight ratio of the active materials. Consequently, SnO_2/rGO nanocomposite structures supported graphene supplied beneficial effects to prevent mechanical disintegration and anode pulverization providing satisfactory discharge capacities as high as 578 mAh g^{-1}.

Conclusions

Free-standing SnO_2/rGO nanocomposite electrodes were produced to obtain high-capacity anode material. Microwave-assisted hydrothermal synthesis of SnO_2 nanopowder and its composite with graphene sheets were performed as a cost effective method to investigate the capacity of Li-ion battery's anodes. Structural and electrochemical analyses of SnO_2/rGO nanocomposite free-standing electrodes were conducted. The results showed that both of the 1:1 and 1:2 SnO_2/rGO free-standing composite anodes supplied high capacities after 50 cycles as 530 and 578 mAh g^{-1}, respectively. Even though the capacity value of 1:2 SnO_2/rGO free-standing electrode is better, 1:1 SnO_2/rGO provides higher capacity retention. So, 1:1 SnO_2/rGO seems to give good stability and capacity for further cycles. As a result, this simple method for the design of porous structure of nanocomposite with a high capacity coupled with an excellent cycling performance may open up a new opportunity to produce a high rate capability and cycling stability metal oxide based anode materials for the next generation applications of Li-ion batteries.

Acknowledgements

References

[1] Ye X, Zhang W, Liu Q, Wang S, Yang Y, Wei H. One-step synthesis of Ni-doped SnO_2 nanospheres with enhanced lithium ion storage performance. New J. Chem 2016;39:130-5.

[2] Köse H, Aydın AO, Akbulut H. Free-standing SnO_2/MWCNT nanocomposite anodes produced by different rate spin coatings for Li-ion batteries. Int. J. Hydrogen Energy 2014;39:21435-46.

[3] Wang Z, Zhang H, Li N, Shi Z, Gu Z, Cao G. Laterally Confined Graphene Nanosheets and Graphene/SnO_2 Composites as High-Rate Anode Materials for Lithium-Ion Batteries. Nano Res 2010;3:748–56.

[4] Chang H, Wu H. Graphene-based nanocomposites: preparation, functionalization, and energy and environmental applications. Energy Environ. Sci 2013;6:3483-507.

[5] Cetinkaya T, Ozcan S, Uysal M, Guler MO, Akbulut H. Free-standing flexible graphene oxide paper electrode for rechargeable $Li-O_2$ batteries. J Power Sour 2014;267:140-7.

[6] Mukherjee R, Krishnan R, Lu TM, Koratkar N. Nanostructured Electrodes for High-Power Lithium Ion Batteries. Nano Energy 2012;1:518-33.

[7] Kucinskis G, Bajars G, Kleperis J. Graphene in lithium ion battery cathode materials: A review. J Power Sour 2013;240:66-79.

[8] Köse H., Aydin A. O., Akbulut H. Sol–gel preparation and electrochemical characterization of SnO_2/MWCNTs anode materials for Li-ion batteries. Appl Surf Sci 2013;275:160-7.

[9] Ahn D, Xiao X, Li Y, Sachdev AK, Park HW, YU A, et al. Applying functionalized carbon nanotubes to enhance electrochemical performances of tin oxide composite electrodes for Li-ion battery. J Power Sour 2012;212:66-72.

[10] Zhang H, Song H, Chen X, Zhou J, Zhang H. Preparation and electrochemical performance of SnO_2@carbon nanotube core–shell structure composites as anode material for lithium-ion batteries. Electrochim Acta 2012;59:160-7.

[11] Ahn HJ, Choi HC, Park KW, Kim SB, Sung YE. Investigation of the structural and electrochemical properties of size-controlled SnO_2 nanoparticles. J Phys Chem B 2004;108:9815-20.

[12] Noerochim L, Wang JZ, Chou SL, Li HJ, Liu HK. SnO_2-coated multiwall carbon nanotube composite anode materials for rechargeable lithium-ion batteries. Electrochim Acta 2010;56:314-20.